



Preliminary communication

Discovery of highly potent triazole antifungal derivatives by heterocycle-benzene bioisosteric replacement



Zhigan Jiang¹, Yan Wang¹, Wenya Wang, Shengzheng Wang, Bo Xu, Guorong Fan, Guoqiang Dong, Yang Liu, Jianzhong Yao, Zhenyuan Miao, Wannian Zhang^{**}, Chunquan Sheng^{*}

School of Pharmacy, Second Military Medical University, 325 Guohe Road, Shanghai 200433, People's Republic of China

ARTICLE INFO

Article history:

Received 11 October 2012
Received in revised form
27 February 2013
Accepted 10 April 2013
Available online 17 April 2013

Keywords:

Triazole
Antifungal activity
Bioisosteric replacement

ABSTRACT

On the basis of our previously discovered triazole antifungal lead compounds, heterocycle-benzene bioisosteric replacement was used to improve their pharmacokinetic profile. The designed new triazole derivatives have good antifungal activity toward a wide range of pathogenic fungi. Their binding mode with the target enzyme was clarified by molecular docking. The MIC value of the highly potent compound **8f** against *Candida albicans*, *Candida tropicalis*, and *Cryptococcus neoformans* is 0.016 µg/mL, 0.004 µg/mL, and 0.016 µg/mL, respectively. Moreover, preliminary pharmacokinetic studies revealed that it showed improved oral absorption as compared to the lead compound iodiconazole and deserved for further evaluations.

© 2013 Elsevier Masson SAS. All rights reserved.

1. Introduction

The incidence and mortality of invasive fungal infections are rising dramatically due to the increase in the number of immunocompromised or immunosuppressed individuals including patients receiving cancer chemotherapy or organ transplantation, and patients infected with human immunodeficiency virus [1,2]. The three most common species of human fungal pathogens are *Candida albicans* (mortality rate: 20%–40%) [3], *Cryptococcus neoformans* (mortality rate: 20%–70%) [4] and *Aspergillus fumigatus* (mortality rate: 50%–90%) [3]. Clinically, antifungal agents for the treatment of invasive fungal infections include polyenes (e.g. amphotericin B) [5], triazoles (e.g. fluconazole and itraconazole, see Fig. 1) [6] and candins (e.g. caspofungin and micafungin) [7]. Among them, triazoles are the most widely used antifungal agents because of their high therapeutic index, broad spectrum of activity and more favorable safety profile [8]. However, broad application of them also led to severe drug resistance, which has significantly reduced their clinical efficacy. Therefore, it is highly desirable to develop new

generation of triazole antifungal agents. Numerous efforts have been made to design and synthesize novel antifungal triazoles and the progress in this field can be found in recent reviews [9–11]. Two of them, isavuconazole and albaconazole (Fig. 1), are candidate new drugs under clinical trials.

Triazole antifungal agents act by competitive inhibition of lanosterol 14 α -demethylase (CYP51), a key enzyme in sterol biosynthesis of fungi [12]. In our previous studies, three-dimensional (3D) models of fungal CYP51s were constructed by homology modeling [13–16]. Moreover, highly active triazole analogs were designed and synthesized by our group [15,17–21]. Among them, triazole derivatives shown in Fig. 2 exhibited excellent *in vitro* activity with broad spectrum [17]. However, these triazoles showed low oral bioavailability due to poor water solubility. The heterocycle-benzene bioisosteric replacement is proved to be a useful approach to improve the solubility and pharmacokinetic profile of the lead compound [22–24]. Herein, a series of heterocyclic analogs of the triazoles in Fig. 2 were designed and synthesized. Several target compounds showed excellent antifungal activity with improved oral absorption, which present promising leads for the development of novel antifungal agents.

2. Chemistry

The first step of chemical synthesis is to prepare various chloromethyl heterocycles or bromomethyl heterocycles according to

* Corresponding author. Tel./fax: +86 21 81871239.

** Corresponding author. Tel./fax: +86 21 81870243.

E-mail addresses: zhangwnk@hotmail.com (W. Zhang), shengcq@hotmail.com (C. Sheng).

¹ These two authors contributed equally to this work.

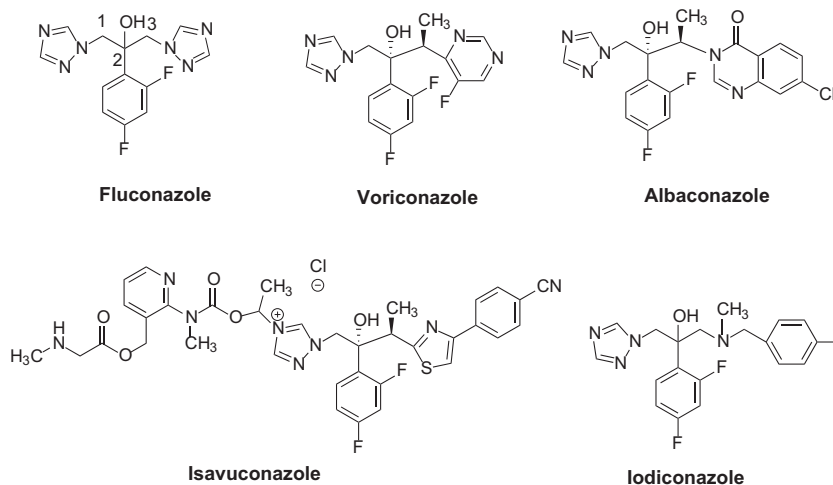


Fig. 1. Chemical structures of representative triazole antifungal agents.

the reported procedures [25,26]. Then, the heterocyclic intermediates were reacted with methylamine or piperazine to give various side chains **5** and **7** (Scheme 1). Finally, the target compounds were obtained as racemates by the ring-open reaction of the oxirane intermediate **4** [18] with intermediates **5** and **7** in the presence of EtOH and a base (Et₃N or K₂CO₃). The isomers of compound **8f** were obtained by chiral HPLC.

3. Microbiology

In vitro antifungal activity was measured according to the National Committee for Clinical Laboratory Standards (NCCLS) recommendations. Serial dilution method in 96-well microtest plate was used to determine the minimum inhibitory concentration (MIC) of the target compounds [18]. Tested fungal strains were obtained from the ATCC or clinical isolates. Briefly, the MIC value was defined as the lowest concentration of tested compounds that resulted in a culture with turbidity less than or equal to 80% inhibition when compared with the growth of the control. Tested compounds were dissolved in DMSO serially diluted in growth medium. The yeasts were incubated at 35 °C and the dermatophytes at 28 °C. Growth MIC was determined at 24 h for *Candida* species, at 72 h for *C. neoformans*, and at 7 days for *A. fumigatus*.

4. Results and discussion

4.1. Design rationale

In our previous studies, we reported a series of new azoles with tertiary amine or piperazine side chains (Fig. 2) [17]. These compounds showed good antifungal activity with a broad spectrum. Among them, iodiconazole was developed as a topical antifungal agent for the treatment of dermatomycosis, which is currently under phase III clinical trial [27–29]. Although iodiconazole has excellent *in vitro* antifungal activity, its oral bioavailability was low mainly because of its poor water solubility. Thus, it is highly desirable to improve its oral absorption and develop novel orally active antifungal agent. In the present investigation, the terminal phenyl group of the lead structures was replaced by various heterocyclic groups to afford target compounds **6a–e** and **8a–f**. This type of bioisosteric replacement was based on the following rationales: (1) the solubility and pharmacokinetic profiles of the compounds should be improved. The heterocycle-benzene exchange is a well-validated approach for the improvement of ADME properties [22]. In particular, this method has been successfully used in the discovery of novel triazole antifungal agents. For example, the replacement of the triazole ring of fluconazole with fluoropyrimidine led to the discovery of voriconazole. Moreover, heterocyclic group seems to be necessary in many marketed or emerging triazole antifungal agents (e.g. voriconazole, isavuconazole, albaconazole, see Fig. 1). The calculated LogP values of compounds **6a–e** and **8a–f** are in the range of 1.92–3.09, suggesting their potential as orally active drugs [30]. (2) Key interactions between the triazole lead and CYP51 should be retained for the bioisosteric replacement. Molecular docking studies revealed that the C3 side chain of the lead compounds (Fig. 2) mainly formed hydrophobic and *van der Waals* interactions with the S4 pocket of *C. albicans* CYP51 (CACYP51) [15]. Analysis of the docking model indicated that five-member or six-member heterocycles and benzoheterocycles can be well accommodated in the active site of CACYP51.

4.2. *In vitro* antifungal activities

In vitro antifungal activity of the target compounds is reported in Table 1. Fluconazole was used as a reference drug. In general, most of the target compounds showed moderate to good inhibitory

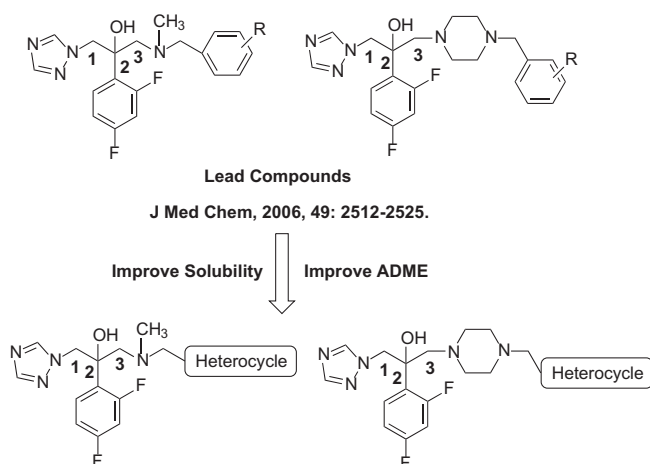
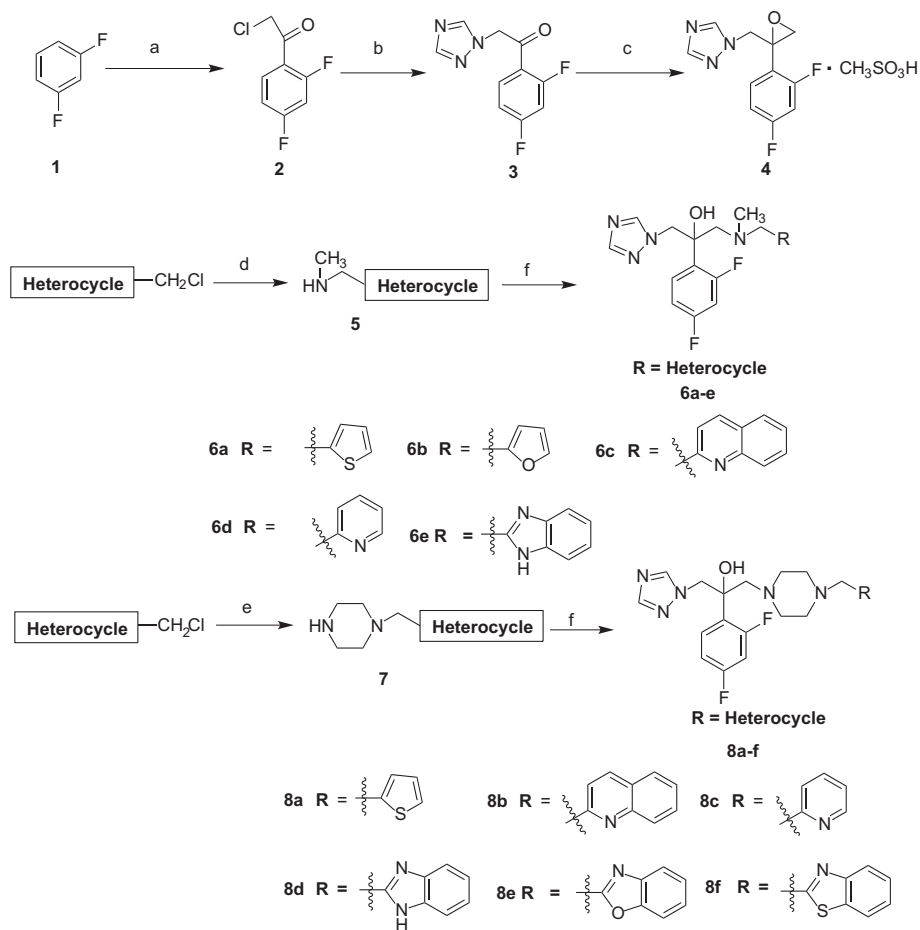


Fig. 2. Design rationale of the target compounds.



Reagents and conditions: a. ClCH_2COCl , AlCl_3 , CH_2Cl_2 , 40°C , 3h, 50%; b. triazole, K_2CO_3 , CH_2Cl_2 , rt, 24h, 70.0%; c. $(\text{CH}_3)_3\text{SOI}$, NaOH , toluene, 60°C , 3h, 62.3%; d. CH_3NH_2 , Et_3N , EtOH , r.t., 12h, ~ 100%; e. piperazine, Et_3N , $n\text{BuOH}$, r.t.~ 80°C , 5h, 95.5%~98.0%; f. **4**, Et_3N , EtOH , 80°C , 9h, 38.8% ~ 76.6%.

Scheme 1.

Table 1
Calculated LogP value and *in vitro* antifungal activities of the target compounds (MIC_{80} , $\mu\text{g mL}^{-1}$).^a

Compd.	LogP ^b	<i>C. alb.</i>	<i>C. tro.</i>	<i>C. neo.</i>	<i>T. rub.</i>	<i>A. fum.</i>
6a	2.60	1	0.125	0.016	1	16
6b	2.04	0.0625	0.016	0.0625	1	64
6c	3.26	4	1	0.25	4	>64
6d	1.92	1	0.0625	0.25	4	>64
6e	2.57	4	0.25	16	>64	>64
8a	2.56	0.0625	0.016	0.25	4	16
8b	3.22	1	0.016	0.0625	0.25	2
8c	1.88	0.0625	1	1	1	16
8d	2.52	4	1	16	64	>64
8e	2.54	0.0625	0.004	0.0625	0.25	0.25
8f	3.09	0.016	0.004	0.016	0.0625	64
Fluconazole	—	0.25	4	2	1	>64

^a Abbreviations: *C. alb.* *Candida albicans*; *C. tro.* *Candida tropicalis*; *C. neo.* *Cryptococcus neoformans*; *T. rub.* *Trichophyton rubrum*; *A. fum.* *Aspergillus fumigatus*.

^b The LogP values were calculated by Discovery Studio 3.0 software package.

activity against the tested fungi, especially for *Candida* species and *C. neoformans*. *Candida* species rank the fourth among the causes of bacterial/fungal nosocomial infectious diseases. The MIC range for *C. albicans* was $4\ \mu\text{g/mL}$ – $0.016\ \mu\text{g/mL}$. Compounds **6b**, **8a**, **8c**, **8e** and **8f** were more active than fluconazole. Among them, compound **8f** ($\text{MIC} = 0.016\ \mu\text{g/mL}$) showed the best activity against *C. albicans*. The target compounds showed better inhibitory activity against *Candida tropicalis* than *C. albicans* with MIC values in the range of $1\ \mu\text{g/mL}$ – $0.004\ \mu\text{g/mL}$. Moreover, all of them were more potent against *C. tropicalis* than fluconazole. Particularly, compounds **8e** and **8f** showed excellent inhibitory activity with MIC value of $0.004\ \mu\text{g/mL}$. *C. neoformans* is the leading cause for cryptococcal meningitis, which kills more than 650,000 people per year worldwide. Good activity of the target compounds was also observed for *C. neoformans* and most compounds had MIC values ranging from $1.0\ \mu\text{g/mL}$ – $0.016\ \mu\text{g/mL}$. Except compounds **6e** and **8d**, the remaining compounds were 2–125 fold more active than fluconazole. Compounds **6a** and **8f** ($\text{MIC} = 0.016\ \mu\text{g/mL}$) revealed the best activity against *C. neoformans*. In contrast, the target compounds showed decreased activity against *Trichophyton rubrum*. Only

compounds **8e** (MIC = 0.25 $\mu\text{g/mL}$) and **8f** (MIC = 0.0625 $\mu\text{g/mL}$) were 4–16 fold more potent than fluconazole (MIC = 1 $\mu\text{g/mL}$). *A. fumigatus* is one of the most common causes of mold infections of humans with high mortality. Fluconazole is inactive against *A. fumigatus*, while several target compounds showed moderate to good activity (MIC range: 0.25 $\mu\text{g/mL}$ –16 $\mu\text{g/mL}$). In particular, compound **8e** was the most active one with MIC value of 0.25 $\mu\text{g/mL}$. Among the synthesized triazoles, compounds **8e** and **8f** showed excellent antifungal activities with a broad spectrum, which represent promising candidates for further pharmacological and pharmacokinetic evaluations. In order to further investigate the influence of the chirality on the antifungal activity, isomers of compound **8f** were prepared by chiral HPLC. The MIC values for isomer (–)-**8f** were lower than 0.016 $\mu\text{g/mL}$ against *C. albicans* and *C. neoformans*, whereas the MIC values for isomer (+)-**8f** were 0.0625 $\mu\text{g/mL}$ and 0.0625 $\mu\text{g/mL}$, respectively. The results indicated that isomer (–)-**8f** had better antifungal activities than isomer (+)-**8f**.

4.3. Structure–activity relationships and molecular docking

From the antifungal activity data, preliminary SARs can be obtained. In general, the amine linker was important for the antifungal activities. Substituted piperazine derivatives were comparable or superior to the corresponding *N*-methyl derivatives. In the *N*-methyl derivatives, the furan derivative **6b** showed the best antifungal activity. Moreover, the furan, thiophene or pyridine group was more favorable for the antifungal activity than the benzoheterocycles (such as benzimidazole and quinoline). For the substituted piperazine derivatives, the SAR of the heterocyclic substitutions was different. Two benzoheterocyclic derivatives, **8e** (benzoxazole) and **8f** (benzothiazole), showed the best antifungal activity. Decreased antifungal activity was observed for the benzimidazole derivative **8d**. In addition, the thiophene group (compound **8a**) was more favorable than the pyridine group (compound **8c**).

In order to investigate the binding mode of the designed compounds with CYP51, two highly potent compounds, **6b** and **8f**, were docked into the homologous model of CACYP51 [13,16]. As shown in Fig. 3, the triazole ring of compounds **6b** and **8f** interacted with the heme group through the formation of a coordination bond with the iron atom. Their difluorophenyl group formed hydrophobic interactions with Phe126, Met306, and Tyr132. The side chain of the two compounds was extended into the S4 pocket of the

CACYP51 active site, but their interactions with CACYP51 were different. The furan ring of compound **6b** formed face to edge π – π interaction with Tyr118 and hydrophobic interactions with Phe380 and Leu121. The side chain of compound **6b** is longer than that of compound **8f**. The piperazine group formed hydrophobic and *van der Waals* interactions with Tyr118 and Met508. The terminal benzothiazole group interacts with surrounding residues Leu121, Phe233, Phe380, and Met508 through hydrophobic contacts. Because compound **8f** (GOLD fitness score: 81.92) had larger docking scores than compound **6b** (GOLD fitness score: 69.23), compound **8f** might have higher binding affinity with CACYP51 and thus showed better inhibitory activity against *C. albicans*.

4.4. Preliminary pharmacokinetic profile of compound **8f**

In order to investigate the pharmacokinetic profile of the designed compounds, compound **8f** was orally administrated to SD rats at the dose of 15 mg/kg and iodiconazole was used as a reference drug. Blood sample from orbital venous plexus was obtained at different time point and subjected to LC/MS/MS analysis (detailed analysis and experimental protocols to be published). Preliminary pharmacokinetic parameters revealed that compound **8f** had better oral absorption than iodiconazole, which further validated the feasibility of the design rationale. The C_{max} and $\text{AUC}_{0-\infty}$ value of compound **8f** were 508.25 ± 101.25 ng/mL and 1421.8 ± 406.98 ng h/mL, respectively, while the two parameters for iodiconazole was 297.11 ± 112.73 ng/mL and 545.79 ± 177.96 ng h/mL. The half-time of compound **8f** ($T_{\text{max}} = 0.8 \pm 0.2$ h, $T_{1/2} = 1.27 \pm 0.5$ h) was similar to that of iodiconazole ($T_{\text{max}} = 0.9 \pm 0.1$ h, $T_{1/2} = 1.38 \pm 0.91$ h). Further pharmacokinetic and pharmacological evaluations are in progress.

5. Conclusion

Heterocycle-benzene exchange was used to improve the pharmacokinetic profile of our previously identified triazole antifungal agents. The designed triazole derivatives showed good antifungal activity with a broad spectrum. The binding mode of them was analyzed by molecular docking. Several compounds, such as **8e** and **8f**, showed significantly higher antifungal activity than fluconazole, which represent promising leads for the development of novel antifungal agents. Preliminary pharmacokinetic profile of compound **8f** was consistent with the design rationale and it

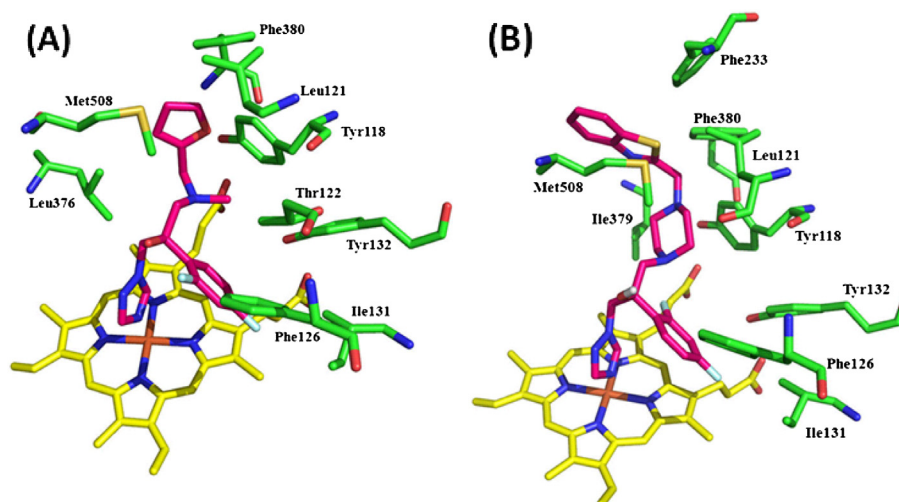


Fig. 3. The binding mode of compound **6b** (A) and **8f** (B) in the active site of CACYP51.

showed better oral absorption than the lead compound iodiconazole.

6. Experimental protocols

6.1. General procedure for the synthesis of compounds

Nuclear magnetic resonance (NMR) spectra were recorded on a Bruker 300 or 500 spectrometer with TMS as an internal standard and CDCl_3 as solvent. Chemical shifts (δ values) and coupling constants (J values) are given in ppm and Hz, respectively. ESI mass spectra were performed on an API-3000 LC-MS spectrometer. IR was performed on Thermo FT-IR (Nicolet 380). Melting points were carried out on OptiMelt MPA100. TLC analysis was carried out on silica gel plates GF254 (Qingdao Haiyang Chemical, China). Silica gel column chromatography was performed with Silica gel 60 G (Qingdao Haiyang Chemical, China). Commercial solvents were used without any pretreatment. The conditions for chiral separation were as follows: Chiralpak AD-3 50×4.6 mm I.D.; $3 \mu\text{m}$ Mobile phase: methanol (0.05% DEA) in CO_2 from 5% to 40%; flow rate: 4 mL/min; wavelength: 220 nm.

6.1.1. Chemical synthesis of *N*-methyl-1-(thiophen-2-yl)methanamine (**5a**)

To a cooled solution of methylamine in EtOH (50 mL) at 0°C was added dropwise a solution of 2-(chloromethyl)thiophene (3.32 g, 0.025 mol) in EtOH (20 mL). Then the reaction mixture was stirred at room temperature overnight. After the reaction was complete, the solvent was removed under reduced pressure to provide a yellow solid, which was used in next step without further purification. ^1H NMR (300 MHz, CDCl_3 , TMS): δ 2.48 (s, 3H), 3.95 (s, 2H), 6.96–7.23 (m, 3H).

The synthetic procedure for other *N*-methyl heterocyclic analogs was similar to the synthesis of compound **5a**.

6.1.2. Chemical synthesis of 1-(thiophen-2-ylmethyl)piperazine (**7a**)

A solution of 2-(chloromethyl)thiophene (3.0 g, 0.023 mol) in *n*-butanol (30 mL) was added dropwise to the suspension of anhydrous piperazine (12.0 g, 0.94 mmol), K_2CO_3 (4.0 g, 29.0 mmol) and *n*-butanol (30 mL) at 0°C . The resulting mixture was stirred at room temperature for 3 h and then heated to 80°C for another 2 h. The reaction mixture was cooled down and filtered. After evaporation, the resulting residue was partitioned between EtOAc and H_2O . The organic layer was dried and evaporated to give a yellow oil, which was used in next step reaction without further purification (4.0 g, yield 95.5%). ^1H NMR (300 MHz, CDCl_3 , TMS): δ 2.48 (m, 4H), 2.84 (m, 4H), 3.60 (s, 2H), 6.83 (d, $J = 7.5$ Hz, 1H), 6.86 (t, $J = 7.5$ Hz, 1H), 7.15 (t, $J = 7.5$ Hz, 1H).

The synthetic procedure for other piperazine analogs was similar to the synthesis of compound **7a**.

6.1.3. 2-(2,4-Difluorophenyl)-1-(methyl(thiophen-2-ylmethyl)amino)-3-(1*H*-1,2,4-triazol-1-yl)propan-2-ol (**6a**)

A solution of epoxide **4** (1.67 g, 0.005 mol), intermediate **5a** (0.76 g, 0.006 mol) and triethylamine (3.0 mL) in EtOH (30 mL) were heated to reflux for 9 h. The solvent was evaporated under reduced pressure. The residue was purified by silica gel column chromatography (eluent: petroleum ether:EtOAc = 1:1, v/v) to give a pale yellow solid (0.94 g, yield 51.8%): mp 86 – 87°C . ^1H NMR (500 MHz, CDCl_3 , TMS): δ 2.10 (s, 3H), 2.80 (d, $J = 13.5$ Hz, 1H), 3.08 (d, $J = 13.5$ Hz, 1H), 3.62 (d, $J = 14.0$ Hz, 2H), 4.46 (d, $J = 14.2$ Hz, 1H), 4.52 (d, $J = 14.2$ Hz, 1H), 5.20 (s, 1H), 6.76–7.61 (m, 6H), 7.75 (s, 1H), 8.10 (s, 1H). ^{13}C NMR (125 MHz, CDCl_3): δ 161.90, 159.85, 150.80, 145.20, 142.25, 130.02, 126.75, 126.30, 125.90, 125.58, 111.00, 104.35,

75.80, 62.75, 57.00, 56.20, 43.90. IR (neat) 3156, 3103, 2839, 2788, 1613, 1518, 1500, 1452, 1279, 1133, 1126, 1142, 1037, 854, 720, 700, 678 cm^{-1} . ESI-MS (m/z): 365.38 [$M + 1$].

6.1.4. 2-(2,4-Difluorophenyl)-1-((furan-2-ylmethyl)(methyl)amino)-3-(1*H*-1,2,4-triazol-1-yl)propan-2-ol (**6b**)

Yellow oil: 1.14 g, yield 65.3%. ^1H NMR (500 MHz, CDCl_3 , TMS): δ 2.17 (s, 3H), 2.80 (d, $J = 13.9$ Hz, 1H), 2.90 (d, $J = 14.9$ Hz, 1H), 3.53 (d, $J = 14.0$ Hz, 2H), 4.46 (d, $J = 14.3$ Hz, 1H), 4.52 (d, $J = 14.3$ Hz, 1H), 5.64 (s, 1H), 6.18–7.56 (m, 6H), 7.71 (s, 1H), 8.27 (s, 1H). ^{13}C NMR (125 MHz, CDCl_3): δ 162.60, 158.92, 152.35, 151.80, 142.75, 130.40, 130.32, 126.45, 111.10, 110.60, 109.10, 104.15, 75.20, 62.15, 55.80, 54.70, 44.08. ESI-MS (m/z): 349.18 [$M + 1$].

6.1.5. 2-(2,4-Difluorophenyl)-1-(methyl(quinolin-2-ylmethyl)amino)-3-(1*H*-1,2,4-triazol-1-yl)propan-2-ol (**6c**)

Pale yellow oil: 1.13 g, yield 55.3%. ^1H NMR (500 MHz, CDCl_3 , TMS): δ 2.21 (s, 3H), 2.89 (d, $J = 14.0$ Hz, 1H), 3.24 (d, $J = 14.0$ Hz, 1H), 3.94 (d, $J = 15.7$ Hz, 2H), 4.48 (d, $J = 14.0$ Hz, 1H), 4.59 (d, $J = 14.0$ Hz, 1H), 5.30 (s, 1H), 6.78–8.14 (m, 9H), 7.57 (s, 1H), 8.16 (s, 1H). ^{13}C NMR (125 MHz, CDCl_3): δ 161.42, 158.50, 157.83, 150.70, 147.01, 144.60, 137.08, 130.41, 130.06, 128.31, 127.64, 127.26, 126.65, 126.1, 120.45, 111.42, 103.92, 73.84, 64.36, 62.26, 56.75, 45.36. ESI-MS (m/z): 410.29 [$M + 1$].

6.1.6. 2-(2,4-Difluorophenyl)-1-(methyl(pyridin-2-ylmethyl)amino)-3-(1*H*-1,2,4-triazol-1-yl)propan-2-ol (**6d**)

Yellow solid: 1.08 g, yield 60.1%, mp 97 – 98°C . ^1H NMR (500 MHz, CDCl_3 , TMS): δ 2.13 (s, 3H), 2.83 (d, $J = 13.95$ Hz, 1H), 3.17 (d, $J = 13.95$ Hz, 1H), 3.66 (d, $J = 14.6$ Hz, 1H), 3.75 (d, $J = 14.6$ Hz, 1H), 4.43 (d, $J = 14.1$ Hz, 1H), 4.57 (d, $J = 14.1$ Hz, 1H), 6.79–7.68 (m, 7H), 7.69 (s, 1H), 8.13 (s, 1H), 8.53 (m, 1H). ^{13}C NMR (125 MHz, CDCl_3): δ 162.35, 159.85, 159.10, 150.75, 148.75, 145.55, 137.05, 130.25, 126.75, 122.65, 122.30, 111.05, 104.00, 75.05, 64.15, 63.05, 56.05, 42.25. IR (neat) 3065, 3033, 3019, 2845, 2807, 2788, 1611, 1597, 1573, 1505, 1460, 1432, 1420, 1272, 1137, 963, 760, 680, 655 cm^{-1} . ESI-MS (m/z): 360.31 [$M + 1$].

6.1.7. 1-(((1*H*-Benzo[d]imidazol-2-yl)methyl)(methyl)amino)-2-(2,4-difluorophenyl)-3-(1*H*-1,2,4-triazol-1-yl)propan-2-ol (**6e**)

Yellow solid: 0.91 g, yield 45.5%, mp 101 – 102°C . ^1H NMR (500 MHz, CDCl_3 , TMS): δ 2.20 (s, 3H), 2.96 (d, $J = 13.9$ Hz, 1H), 3.17 (d, $J = 13.9$ Hz, 1H), 3.47 (d, $J = 14.5$ Hz, 1H), 3.66 (d, $J = 14.5$ Hz, 1H), 4.57 (d, $J = 14.0$ Hz, 2H), 6.75–7.76 (m, 7H), 7.72 (s, 1H), 8.08 (s, 1H). ^{13}C NMR (125 MHz, CDCl_3): δ 162.10, 159.65, 152.75, 150.65, 145.75, 143.00, 134.35, 130.03, 126.15, 122.25, 121.65, 118.45, 111.50, 111.30, 104.25, 75.10, 63.00, 56.45, 56.02, 44.60. IR (neat) 3400, 3123, 2954, 1615, 1497, 1455, 1418, 1271, 1135, 964, 849, 743, 676 cm^{-1} . ESI-MS (m/z): 399.29 [$M + 1$].

6.1.8. 2-(2,4-Difluorophenyl)-1-(4-(thiophen-2-ylmethyl)piperazin-1-yl)-3-(1*H*-1,2,4-triazol-1-yl)propan-2-ol (**8a**)

A solution of epoxide **4** (1.67 g, 0.005 mol), 1-(thiophen-2-ylmethyl)piperazine (1.09 g, 0.006 mol) and triethylamine (2.0 mL) in anhydrous EtOH (20 mL) were heated to reflux for 8 h. The solvent was evaporated under reduced pressure. The residue was purified by silica gel column chromatography (eluent: petroleum ether:EtOAc = 1:1, v/v) to give a yellow oil (1.22 g, yield 58.2%). ^1H NMR (500 MHz, CDCl_3 , TMS): δ 2.36 (s, 8H), 2.65 (d, $J = 13.5$ Hz, 1H), 3.07 (d, $J = 13.5$ Hz, 1H), 3.65 (dd, $J_1 = 13.8$ Hz, $J_2 = 21.9$ Hz, 2H), 4.50 (dd, $J_1 = 14.3$ Hz, $J_2 = 18.0$ Hz, 2H), 5.30 (s, 1H), 6.77–7.54 (m, 6H), 7.77 (s, 1H), 8.14 (s, 1H). ^{13}C NMR (125 MHz, CDCl_3): δ 162.04, 159.61, 151.01, 144.64, 141.12, 129.25, 126.41, 126.23, 126.11, 125.08, 111.61, 104.26, 71.83, 62.16, 56.87, 56.38, 54.27, 52.68. ESI-MS (m/z): 420.24 [$M + 1$].

6.1.9. 2-(2,4-Difluorophenyl)-1-(4-(quinolin-2-ylmethyl)piperazin-1-yl)-3-(1H-1,2,4-triazol-1-yl)propan-2-ol (**8b**)

Yellow oil: 1.45 g, yield 62.3%. ¹H NMR (500 MHz, CDCl₃, TMS): δ 2.34–2.44 (m, 8H), 2.65 (d, *J* = 13.5 Hz, 1H), 3.09 (d, *J* = 13.5 Hz, 1H), 3.78 (dd, *J*₁ = 13.8 Hz, *J*₂ = 17.4 Hz, 2H), 4.51 (t, *J* = 15.6 Hz, 2H), 5.30 (s, 1H), 6.75–8.06 (m, 9H), 8.08 (s, 1H), 8.11 (s, 1H). ¹³C NMR (125 MHz, CDCl₃): δ 162.70, 159.52, 159.04, 151.00, 147.61, 144.65, 136.35, 129.39, 129.30, 129.04, 127.48, 127.32, 126.30, 126.19, 120.99, 111.60, 104.21, 71.88, 64.93, 62.22, 56.35, 54.28, 53.31. ESI-MS (*m/z*): 465.30 [M + 1].

6.1.10. 2-(2,4-Difluorophenyl)-1-(4-(pyridin-2-ylmethyl)piperazin-1-yl)-3-(1H-1,2,4-triazol-1-yl)propan-2-ol (**8c**)

Pale yellow oil: 1.24 g, yield 60.1%. ¹H NMR (500 MHz, CDCl₃, TMS): δ 2.30–2.39 (m, 8H), 2.65 (d, *J* = 13.5 Hz, 1H), 3.08 (d, *J* = 13.5 Hz, 1H), 3.62 (d–d, *J*₁ = 13.5 Hz, *J*₂ = 17.7 Hz, 2H), 4.51 (t, *J* = 4.4 Hz, 2H), 6.75–7.78 (m, 7H), 7.92 (s, 1H), 8.15 (s, 1H). ¹³C NMR (125 MHz, CDCl₃): δ 162.03, 160.69, 158.15, 151.05, 149.33, 144.67, 136.36, 129.35, 126.26, 123.19, 122.10, 111.64, 104.26, 71.87, 64.37, 62.26, 56.38, 54.25, 53.30. ESI-MS (*m/z*): 415.10 [M + 1].

6.1.11. 1-(4-((1H-Benzod[imidazol-2-yl)methyl]piperazin-1-yl)-2-(2,4-difluoro phenyl)-3-(1H-1,2,4-triazol-1-yl)propan-2-ol (**8d**)

Yellow solid: 1.04 g, yield 45.7%, 134–135 °C. ¹H NMR (500 MHz, CDCl₃, TMS): δ 2.42–2.47 (m, 8H), 2.66 (d, *J* = 13.5 Hz, 1H), 3.09 (d, *J* = 13.5 Hz, 1H), 3.80 (dd, *J*₁ = 14.7 Hz, *J*₂ = 15.6 Hz, 2H), 4.52 (dd, *J*₁ = 14.4 Hz, *J*₂ = 18.6 Hz, 2H), 6.75–7.79 (m, 7H), 7.81 (s, 1H), 8.17 (s, 1H). ¹³C NMR (125 MHz, CDCl₃): δ 163.25, 160.80, 158.20, 152.00, 151.05, 145.25, 130.35, 126.45, 121.80, 110.10, 104.10, 75.00, 64.05, 56.00, 54.35, 53.10. IR (neat) 3280, 3053, 2702, 1559, 1385, 1305, 1182, 1050, 909, 705 cm⁻¹. ESI-MS (*m/z*): 454.24 [M + 1].

6.1.12. 1-(4-(Benzo[d]oxazol-2-ylmethyl)piperazin-1-yl)-2-(2,4-difluorophenyl)-3-(1H-1,2,4-triazol-1-yl)propan-2-ol (**8e**)

Brown oil: 1.64 g, yield 72.1%. ¹H NMR (500 MHz, CDCl₃, TMS): δ 2.43–2.49 (m, 8H), 2.66 (d, *J* = 13.2 Hz, 1H), 3.09 (d, *J* = 13.2 Hz, 1H), 3.82 (d–d, *J*₁ = 14.4 Hz, *J*₂ = 15.6 Hz, 2H), 4.48 (dd, *J*₁ = 13.8 Hz, *J*₂ = 17.1 Hz, 2H), 5.27 (s, 1H), 6.76–7.72 (m, 7H), 7.78 (s, 1H), 8.14 (s, 1H). ¹³C NMR (125 MHz, CDCl₃): δ 162.67, 162.35, 159.55, 1051.06, 150.87, 144.63, 140.89, 129.34, 126.14, 125.16, 124.41, 120.08, 111.70, 110.73, 104.30, 72.02, 62.25, 60.37, 55.02, 54.09, 53.05. ESI-MS (*m/z*): 455.10 [M + 1].

6.1.13. 1-(4-(Benzo[d]thiazol-2-ylmethyl)piperazin-1-yl)-2-(2,4-difluorophenyl)-3-(1H-1,2,4-triazol-1-yl)propan-2-ol (**8f**)

White solid: 1.58 g, yield 67.2%, 122–123 °C. ¹H NMR (500 MHz, CDCl₃, TMS): δ 2.43–2.54 (m, 8H), 2.68 (d, *J* = 13.2 Hz, 1H), 3.12 (d, *J* = 13.2 Hz, 1H), 3.90 (dd, *J*₁ = 15.0 Hz, *J*₂ = 16.5 Hz, 2H), 4.52 (dd, *J*₁ = 14.1 Hz, *J*₂ = 17.7 Hz, 2H), 5.31 (s, 1H), 6.76–7.96 (m, 7H), 7.79 (s, 1H), 8.15 (s, 1H). ¹³C NMR (125 MHz, CDCl₃): δ 171.41, 162.21, 159.76, 153.23, 151.10, 144.68, 135.34, 129.36, 126.28, 125.88, 124.95, 122.85, 121.66, 111.60, 104.30, 72.02, 62.22, 60.00, 56.29, 54.29, 53.30. ESI-MS (*m/z*): 471.30 [M + 1].

6.1.14. (+)-1-(4-(Benzo[d]thiazol-2-ylmethyl)piperazin-1-yl)-2-(2,4-difluorophenyl)-3-(1H-1,2,4-triazol-1-yl)propan-2-ol ((+)-**8f**)

¹H NMR (500 MHz, CDCl₃): δ 2.32–2.62 (m, 8H), 2.70 (d, *J* = 13.6 Hz, 1H), 3.13 (d, *J* = 13.6 Hz, 1H), 3.86–3.98 (m, 2H), 4.49–4.61 (m, 2H), 5.23 (br s, 1H), 6.77–6.86 (m, 2H), 7.34–7.42 (m, 1H), 7.43–7.51 (m, 1H), 7.52–7.61 (m, 1H), 7.81 (s, 1H), 7.86 (d, *J* = 7.8 Hz, 1H), 7.97 (d, *J* = 8.0 Hz, 1H), 8.17 (s, 1H). IR (neat) 3374, 2937, 2816, 1615, 1596, 1497, 1456, 1420, 1333, 1270, 1159, 1135, 1010, 963, 849, 830, 759, 730, 678, 665 cm⁻¹. ESI-MS (*m/z*): 470.25 [M + 1]. [α]_D²⁰ = +14.0 (C = 0.1, DMF), 98.6% ee.

6.1.15. (–)-1-(4-(Benzo[d]thiazol-2-ylmethyl)piperazin-1-yl)-2-(2,4-difluorophenyl)-3-(1H-1,2,4-triazol-1-yl)propan-2-ol ((–)-**8f**)

¹H NMR (500 MHz, CDCl₃): δ 2.33–2.63 (m, 8H), 2.70 (d, *J* = 13.6 Hz, 1H), 3.13 (d, *J* = 13.6 Hz, 1H), 3.87–3.97 (m, 2H), 4.49–4.60 (m, 2H), 5.23 (br s, 1H), 6.77–6.86 (m, 2H), 7.35–7.41 (m, 1H), 7.43–7.49 (m, 1H), 7.53–7.60 (m, 1H), 7.81 (s, 1H), 7.86 (d, *J* = 8.0 Hz, 1H), 7.97 (d, *J* = 8.0 Hz, 1H), 8.17 (s, 1H). IR (neat) 3425, 3130, 2934, 2820, 1615, 1596, 1510, 1495, 1422, 1360, 1270, 1153, 1134, 1120, 1011, 964, 854, 756, 688, 655 cm⁻¹. ESI-MS (*m/z*): 470.20 [M + 1]. [α]_D²⁰ = –16.0 (C = 0.1, DMF), 97.2% ee.

6.2. Molecular docking

Our previous study indicated that GOLD [31] is an accurate method to dock CYP51 inhibitors [8]. Homology model of CACYP51 [15] from our group was used for molecular docking and the docking parameters were defined the same with our previous reports [8].

Acknowledgments

This work was supported by the National Natural Science Foundation of China (Grant 30930107, 81222044), Key Project of Science and Technology of Shanghai (No. 10431902100), the 863 Hi-Tech Program of China (Grant 2012AA020302), Shanghai Rising-Star Program (grant 12QH1402600) and Shanghai Municipal Health Bureau (Grant XYQ2011038).

References

- [1] J.J. Caston-Osorio, A. Rivero, J. Torre-Cisneros, Epidemiology of invasive fungal infection, *Int. J. Antimicrob. Agents* 32 (Suppl. 2) (2008) S103–S109.
- [2] M. Cuenca-Estrella, L. Bernal-Martinez, M.J. Buitrago, M.V. Castelli, A. Gomez-Lopez, O. Zaragoza, J.L. Rodriguez-Tudela, Update on the epidemiology and diagnosis of invasive fungal infection, *Int. J. Antimicrob. Agents* 32 (Suppl. 2) (2008) S143–S147.
- [3] C.C. Lai, C.K. Tan, Y.T. Huang, P.L. Shao, P.R. Hsueh, Current challenges in the management of invasive fungal infections, *J. Infect. Chemother.* 14 (2008) 77–85.
- [4] B.J. Park, K.A. Wannemuehler, B.J. Marston, N. Govender, P.G. Pappas, T.M. Chiller, Estimation of the current global burden of cryptococcal meningitis among persons living with HIV/AIDS, *AIDS* 23 (2009) 525–530.
- [5] L. Ostrosky-Zeichner, K.A. Marr, J.H. Rex, S.H. Cohen, Amphotericin B: time for a new “gold standard”, *Clin. Infect. Dis.* 37 (2003) 415–425.
- [6] G. Aperis, E. Mylonakis, Newer triazole antifungal agents: pharmacology, spectrum, clinical efficacy and limitations, *Expert Opin. Investig. Drugs* 15 (2006) 579–602.
- [7] C.A. Kauffman, P.L. Carver, Update on echinocandin antifungals, *Semin. Respir. Crit. Care Med.* 29 (2008) 211–219.
- [8] S. Wang, G. Jin, W. Wang, L. Zhu, Y. Zhang, G. Dong, Y. Liu, C. Zhuang, Z. Miao, J. Yao, W. Zhang, C. Sheng, Design, synthesis and structure–activity relationships of new triazole derivatives containing N-substituted phenoxypipylamino side chains, *Eur. J. Med. Chem.* 53 (2012) 292–299.
- [9] C. Sheng, W. Zhang, New lead structures in antifungal drug discovery, *Curr. Med. Chem.* 18 (2011) 733–766.
- [10] K. Shalini, N. Kumar, S. Drabu, P.K. Sharma, Advances in synthetic approach to and antifungal activity of triazoles, *Beilstein J. Org. Chem.* 7 (2011) 668–677.
- [11] C.H. Zhou, Y. Wang, Recent researches in triazole compounds as medicinal drugs, *Curr. Med. Chem.* 19 (2012) 239–280.
- [12] Y. Aoyama, Y. Yoshida, R. Sato, Yeast cytochrome P-450 catalyzing lanosterol 14 alpha-demethylation. II. Lanosterol metabolism by purified P-450(14)DM and by intact microsomes, *J. Biol. Chem.* 259 (1984) 1661–1666.
- [13] H. Ji, W. Zhang, Y. Zhou, M. Zhang, J. Zhu, Y. Song, J. Lu, A three-dimensional model of lanosterol 14alpha-demethylase of *Candida albicans* and its interaction with azole antifungals, *J. Med. Chem.* 43 (2000) 2493–2505.
- [14] C. Sheng, Z. Miao, H. Ji, J. Yao, W. Wang, X. Che, G. Dong, J. Lu, W. Guo, W. Zhang, Three-dimensional model of lanosterol 14 alpha-demethylase from *Cryptococcus neoformans*: active-site characterization and insights into azole binding, *Antimicrob. Agents Chemother.* 53 (2009) 3487–3495.
- [15] C. Sheng, W. Wang, X. Che, G. Dong, S. Wang, H. Ji, Z. Miao, J. Yao, W. Zhang, Improved model of lanosterol 14alpha-demethylase by ligand-supported homology modeling: validation by virtual screening and azole optimization, *ChemMedChem* 5 (2010) 390–397.
- [16] C. Sheng, W. Zhang, M. Zhang, Y. Song, H. Ji, J. Zhu, J. Yao, J. Yu, S. Yang, Y. Zhou, J. Lu, Homology modeling of lanosterol 14alpha-demethylase of *Candida albicans* and *Aspergillus fumigatus* and insights into the enzyme–substrate interactions, *J. Biomol. Struct. Dyn.* 22 (2004) 91–99.

- [17] X. Che, C. Sheng, W. Wang, Y. Cao, Y. Xu, H. Ji, G. Dong, Z. Miao, J. Yao, W. Zhang, New azoles with potent antifungal activity: design, synthesis and molecular docking, *Eur. J. Med. Chem.* 44 (2009) 4218–4226.
- [18] C. Sheng, W. Zhang, H. Ji, M. Zhang, Y. Song, H. Xu, J. Zhu, Z. Miao, Q. Jiang, J. Yao, Y. Zhou, J. Lu, Structure-based optimization of azole antifungal agents by CoMFA, CoMSIA, and molecular docking, *J. Med. Chem.* 49 (2006) 2512–2525.
- [19] W. Wang, C. Sheng, X. Che, H. Ji, Y. Cao, Z. Miao, J. Yao, W. Zhang, Discovery of highly potent novel antifungal azoles by structure-based rational design, *Bioorg. Med. Chem. Lett.* 19 (2009) 5965–5969.
- [20] W. Wang, C. Sheng, X. Che, H. Ji, Z. Miao, J. Yao, W.N. Zhang, Design, synthesis, and antifungal activity of novel conformationally restricted triazole derivatives, *Arch. Pharm. (Weinheim)* 342 (2009) 732–739.
- [21] Y. Xu, C. Sheng, W. Wang, X. Che, Y. Cao, G. Dong, S. Wang, H. Ji, Z. Miao, J. Yao, W. Zhang, Structure-based rational design, synthesis and antifungal activity of oxime-containing azole derivatives, *Bioorg. Med. Chem. Lett.* 20 (2010) 2942–2945.
- [22] N.A. Meanwell, Synopsis of some recent tactical application of bioisosteres in drug design, *J. Med. Chem.* 54 (2011) 2529–2591.
- [23] L.M. Lima, E.J. Barreiro, Bioisosterism: a useful strategy for molecular modification and drug design, *Curr. Med. Chem.* 12 (2005) 23–49.
- [24] G.A. Patani, E.J. LaVoie, Bioisosterism: a rational approach in drug design, *Chem. Rev.* 96 (1996) 3147–3176.
- [25] J. Hou, Z. Tan, Y. Yan, Y. He, C. Yang, Y. Li, Synthesis and photovoltaic properties of two-dimensional conjugated polythiophenes with bi(thienylenevinylene) side chains, *J. Am. Chem. Soc.* 128 (2006) 4911–4916.
- [26] C. Sheng, X. Che, W. Wang, S. Wang, Y. Cao, J. Yao, Z. Miao, W. Zhang, Design and synthesis of antifungal benzoheterocyclic derivatives by scaffold hopping, *Eur. J. Med. Chem.* 46 (2011) 1706–1712.
- [27] N. Sun, J. Wen, G. Lu, Z. Hong, G. Fan, Y. Wu, C. Sheng, W. Zhang, An ultra-fast LC method for the determination of iodiconazole in microdialysis samples and its application in the calibration of laboratory-made linear probes, *J. Pharm. Biomed. Anal.* 51 (2010) 248–251.
- [28] S. Gao, X. Tao, L. Sun, C. Sheng, W. Zhang, Y. Yun, J. Li, H. Miao, W. Chen, An liquid chromatography-tandem mass spectrometry assay for determination of trace amount of new antifungal drug iodiconazole in human plasma, *J. Chromatogr. B. Analyt. Technol. Biomed. Life Sci.* 877 (2009) 382–386.
- [29] J. Wen, G.R. Fan, Z.Y. Hong, Y.F. Chai, X.P. Yin, Y.T. Wu, C.Q. Sheng, W.N. Zhang, High performance liquid chromatographic determination of a new antifungal compound, ADKZ in rat plasma, *J. Pharm. Biomed. Anal.* 43 (2007) 655–658.
- [30] C.A. Lipinski, F. Lombardo, B.W. Dominy, P.J. Feeney, Experimental and computational approaches to estimate solubility and permeability in drug discovery and development settings, *Adv. Drug Deliv. Rev.* 46 (2001) 3–26.
- [31] G. Jones, P. Willett, R.C. Glen, A.R. Leach, R. Taylor, Development and validation of a genetic algorithm for flexible docking, *J. Mol. Biol.* 267 (1997) 727–748.